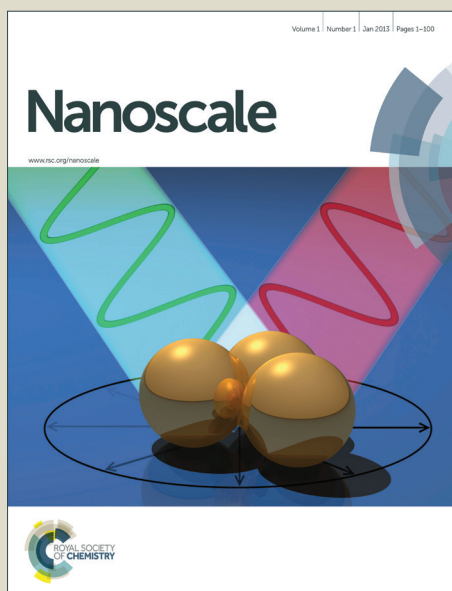# Nanoscale

Accepted Manuscript

This is an *Accepted Manuscript*, which has been through the Royal Society of Chemistry peer review process and has been accepted for publication.

Accepted Manuscripts are published online shortly after acceptance, before technical editing, formatting and proof reading. Using this free service, authors can make their results available to the community, in citable form, before we publish the edited article. We will replace this *Accepted Manuscript* with the edited and formatted *Advance Article* as soon as it is available.

You can find more information about *Accepted Manuscripts* in the **Information for Authors**.

Real-Time Investigation of Human Topoisomerase I Reaction Kinetics using an Optical Sensor: A Fast Method for Drug Screening and Determination of Active Enzyme Concentrations.

Emil L. Kristoffersen[1,2], Line A. Jørgensen[1], Oskar Franch[1,2], Michael Etzerodt[1], Rikke Frøhlich[1], Lotte Bjergbæk[1], Magnus Stougaard[3,2], Yi-Ping Ho[1,2], Birgitta R. Knudsen[1,2#]

[1]Department of Molecular Biology and Genetics, Aarhus University, Denmark

[2]Interdisciplinary Nanoscience Center (iNANO), Aarhus University, Denmark

[3]Department of Pathology, Aarhus University Hospital, Denmark

[#]Corresponding author. Contact information: brk@mbg.au.dk

Abstract:

Human DNA topoisomerase I (hTopI) is a nuclear enzyme that catalyzes relaxation of super helical tension that arises in the genome during essential DNA metabolic processes. This is accomplished through a common reaction mechanism shared among the type IB topoisomerase enzymes, including eukaryotic and poxvirus topoisomerase I. The mechanism of hTopI is specifically targeted in cancer treatment using camptothecin derivatives. These drugs convert the hTopI activity into a cellular poison, and hence the cytotoxic effects of camptothecin derivatives correlate with the hTopI activity. Therefore, fast and reliable techniques for high throughput measurements of hTopI activity are of high clinical interest. Here we demonstrate potential applications of a fluorophore-quencher based DNA sensor designed for measurement of hTopI cleavage-ligation activities, which are the catalytic steps affected by camptothecin. The kinetic analysis of the hTopI reaction with the DNA sensor exhibits a characteristic *burst profile*. This is the result of a two-step *ping-pong* reaction mechanism, where a fast first reaction, the one creating the signal, is followed by a slower second reaction necessary for completion of the catalytic cycle. Hence, the burst profile holds information about two reactions in the enzymatic mechanism. Moreover, it allows the amount of active enzyme in the reaction to be determined. The presented results pave the way for future high throughput drug screening and the potential of measuring active hTopI concentrations in clinical samples for individualized treatment.

1.Introduction

During the past decade, chemical synthesis and modification of DNA have become accessible, inexpensive and well characterized. This means that modified DNA sensors are becoming attractive tools for investigation of enzymatic properties for a number of different DNA processing enzymes [1]–[6]. In general, molecular sensors are generated by coupling chemical compounds, usually organic fluorophores, quenchers, chromophores, or even quantum dots and other nanoparticles [3], to a synthetic DNA strand. For example, the specific cleavage reactions performed by enzymes such as endonucleases or tyrosyl-DNA phosphodiesterase 1 (Tdp1) on specially designed DNA sensors can be followed over time due to increased fluorescence upon cleavage of the targeted sensors [1], [6], [7]. The hTopI mediated ligation step has been detected by a quantum dot based DNA sensor [3]. In this way, modified DNA oligonucleotides can be used as real-time sensors for relatively easy, specific and fast investigation of kinetic properties for a range of DNA modifying enzymes [8]–[14]. In line with the above, a fluorophore and quencher coupled DNA sensor have been designed to study the cleavage-ligation reaction of hTopI in real-time [2]. In comparison to the quantum dot based sensor mentioned above, the real-time sensor presented here directly measures the cleavage step of hTopI catalysis based on emission from an organic fluorophore and thus may be more suitable for analysis in crude biological samples, which in some cases may affect the response of quantum dots.

hTopI belongs to the family of eukaryotic type IB topoisomerases, which are part of the cellular toolbox for regulation of the DNA topology. The enzyme relaxes super-helical tension arising in the double helix during cellular DNA metabolic processes, such as replication [15] and transcription [16]. The enzymatic reaction of eukaryotic type IB topoisomerases can be described by a common reaction mechanism, which can be divided into five steps, including: 1) non-covalent DNA binding, 2) single strand DNA cleavage, facilitated by a nucleophilic attack by the active site tyrosine (Tyr723) on the DNA backbone phosphate resulting in the formation of a covalent 3´-phosphotyrosyl cleavage complex, 3) strand rotation, during which topological strain is relieved by rotation of the free 5´-OH-end generated during cleavage around the non-cleaved strand, 4) religation, where the covalent cleavage complex is resolved by the attack of the free 5´-OH-group

reforming the original DNA strand, 5) dissociation and enzyme turnover, where the enzyme dissociates from the DNA [17]. A comprehensive review of the roles and mechanism of type IB topoisomerases can be found in several reviews [18]–[20].

Besides its important cellular functions, hTopI is frequently used as a target in anticancer treatment. Inhibition of the hTopI enzymatic reaction by members of the campthothecin (CPT) family of drugs is applied in chemotherapeutic treatment of various cancers, including colon-, ovarian- and small cell lung cancers [21]–[24]. CPT acts by inhibiting the religation step of hTopI catalysis and thereby stabilizing the transient covalent cleavage complexes [25]. This results in the formation of lethal double stranded DNA breaks upon collision with the replication machinery [25]–[27]. Hence, CPT derivatives convert hTopI into a cell poison and consequently high cleavage activity of hTopI may predict high drug sensitivity of human tumors while reduced hTopI cleavage activity may result in drug resistant cancer.

Motivated by the need of measuring hTopI activity for the purposes of both clinical- and basic science, we previously designed and tested a real-time DNA sensor [2], allowing cleavage by hTopI to be followed over time by an increased fluorescence signal caused by the diffusion of a quencher moiety that was cleaved off. Enzymatic turnover was ensured by the presence of a 5´-OH DNA end that was ligated by hTopI. Note, that the sensor was designed to specifically measure the cleavage-ligation steps of the hTopI reaction, which are the steps affected by CPT. One of the interesting observations in the initial study, which was not analyzed in the initial paper, was the occurrence of a *burst profile* resulting from incubation of hTopI with the sensor. This burst profile, which is the focus of the current study, was characterized by an initial steep increase in fluorescence (until around 1.5 minutes after addition of hTopI), followed by a slower and linear increase in fluorescence (until at least 20 minutes after hTopI addition) termed the *burst phase* and the *steady phase,* respectively. The burst profile is a known kinetic phenomenon characteristic of a specific kind of *ping-pong* mechanism in which a product must be released from the enzyme before the next substrate can react [28], [29]. In other words, the burst profile represents a fast reaction creating the signal followed by a slower reaction necessary for completion of the catalytic cycle. In the current study, we have investigated the burst profile of hTopI in detail using the previously published DNA sensor [2]. We demonstrate that the presented

assay setup provides a simple and relatively fast mean of determining important kinetic constants of hTopI, from the extensive dataset that can be obtained from even a single test tube. The presented results strongly suggest that it is the catalytic steps that succeed DNA cleavage i.e. substrate turnover that is the rate limiting step of hTopI catalysis, while cleavage is relatively fast. This is consistent with previous studies performed on the poxviral type IB topoisomerase, vaccinia virus topoisomerase I (vvTopI) [30], which is often regarded a minimal prototype topoisomerase IB enzyme. Indeed, the burst phase represents the first cleavage reaction performed by each active enzyme and provides a basis of calculating the concentration of active enzyme in the reaction mixture under investigation. Because only active enzymes can be trapped in complex with DNA and thereby contribute to the cytotoxicity of CPT such calculations may provide a new important method to predict chemotherapeutic response.

2. Materials and Methods:

2.1 The kinetic model

The theory used in this paper is inspired by the approach taken up by Stivers *et al.* in 1994 upon studying vvTopI [30] and the work of Fresht, from 1985 [29].

The expression for, *the rate constant of the burst phase* (termed, k_{busrt}), *the rate constant of the steady phase* (termed, k_{steady}), and *the burst amplitude* are defined by the following equations [29]:

Equation 1: $\qquad\qquad v_{burst} = k_{burst}[E]_0 \frac{[S-Q]}{[S-Q]+K_M}$, where $k_{burst} = (k_{cl} + k_2)$

Equation 2: $\qquad\qquad v_{steady} = k_{steady}[E]_0 \frac{[S-Q]}{[S-Q]+K_M}$, where $k_{steady} = \frac{k_2}{1+\frac{k_2}{k_{cl}}}$

Equation 3: $\qquad\qquad burst\ amplitude = [E]_0 \left(\frac{k_{cl}}{k_{cl}+k_2}\right)^2,$

where v_{burst} is the initial velocity of the burst phase, v_{steady} is the steady state velocity of the steady phase, $[E_0]$ is the amount of active enzyme added to the reaction, k_{cl} and k_2 indicates the first order rate constants, [S-Q] is the concentration of the DNA sensor, and K_M is the Michaelis constant.

As shown in figure 1C, the velocity of the reactions can be found by making linear fits to the initial part of the burst phase and the linear part of the steady phase, respectively. From equations 1 and 2 it can be seen that k_{burst} and k_{steady} can be calculated from the velocity of the reaction when this is at maximum, if $[E_0]$ is known. In figure 1C it is shown that the burst amplitude can be found from the y-axis intercept of a linear fit to the steady phase [29].

The relations between k_{cl}, k_2 from the hTopI reaction, and k_{burst}, k_{steady} that can be seen from the burst profile are given by the following equations:

Equation 4:
$$k_{burst} = k_{cl} + k_2$$

Equation 5:
$$k_{steady} = \frac{k_2}{1 + \frac{k_2}{k_{cl}}}$$

Thus, the k_{burst}, k_{steady} and the *burst amplitude* can provide information about, 1) the rate constant of cleavage (k_{cl}), 2) the rate constant of the netto forward reaction (k_2), and 3) the amount of active enzyme in the reaction ($[E_0]$). In the case where k_{cl} is much faster than k_2, k_{burst} will be dominated by k_{cl}, whereas k_{steady} will be dominated by k_2. Finally, as seen from equation 3, the amplitude of the burst phase will be approximately equal to $[E_0]$ when $k_{cl} \gg k_2$.

2.2 Yeast Strains and Construction of hTopI Expression Plasmids

The yeast *Saccharomyces cerevisiae* top1-null strain RS190 was a kind gift from R. Sternglanz (State University of New York, Stony Brook, NY, USA). Plasmid pHT143, for expression of recombinant full-length hTopI, was described previously [31].

2.3 Expression and Purification of hTopI and Preparation of Cell Extracts

The plasmid pHT143 was transformed into the *S. cerevisiae* strain RS190. The cells were grown, and hTopI expression was induced as described by Björnsti *et al*. [32]. Preparation of crude cell extracts and purification of hTopI were conducted as previously described [33]. The protein concentrations were estimated from Coomassie blue-stained SDS-polyacrylamide gels by comparison to serial dilutions of BSA. Western blotting to test the expression level of hTopI in cell extracts was performed essentially as described by Hede *et al*.[34].

2.4 The real-time hTopI assay based on the DNA sensor

The hTopI DNA sensor consists of two oligonucleotides (purchased from DNA-technology, Denmark), the L strand: 5'-AGA AAA ATT TTT ACA GGC CTA GC-C6amine and the Cl strand: 5'-GCT AGG CCT GTA AAA ATT T**T**T CTA AGT CTT TTA GAT CAT CGT TAT TCG ATG ATC TAA AAG ACT **TA**G A-BHQ1. The bold underlined T was labeled with a 6-carboxyfluorescein (FAM), the bold underlined TA indicates the cleavage site, and the Black Hole Quencher 1 (BHQ1) was attached through a phosphorthioate bond. Hybridization of the two oligonucleotides formed the active sensor.

Activity measurements were carried out using the indicated concentrations of DNA sensor and purified hTopI in a total volume of 25 µL containing 1x hTopI buffer (10 mM Tris-HCl pH 7.5, 5 mM $CaCl_2$, 5 mM $MgCl_2$ and 0.1 mM DTT). The noted amount of active hTopI added to each sample was calculated from the total amount of enzyme in the stock and multiplied by the fraction of active hTopI. The calculation of the active hTopI amount is described below.

To be able to measure the very first part of the reaction, the components were mixed in two separate tubes, one containing the substrate and the second containing the enzyme. The tubes were heated up to 37 ^{O}C and mixed immediately before the first measurement took place. Development of fluorescence was followed in a Mx3000P qPCR machine (Agilent Technologies, Inc.) and data were collected every 15 sec. for at least 20 min.

2.5 Conversion curve

In order to be able to convert the units of fluorescence, measured by the qPCR machine, to the amount of product formed, a conversion curve was made. To make the conversion curve, known concentrations of reaction product, which is the DNA sensor without the quencher and tri-nucleotide, was incubated in the reaction buffer and fluorescence was measured. An example of such a conversion curve is shown in supplementary figure 2. The DNA sensor without the quencher and tri-nucleotide, which is equal to the reaction product, noted as P* in figure 1 was purchased from DNA Technology (Denmark).

2.6 Data fitting and kinetic parameter calculation

After conversion of fluorescence signal to product concentration, least square fits were made to 1) the initial three data points, burst phase region, and 2) the data points from 5-10 minutes, steady phase region. The slopes of the fits were plotted as a function of the DNA sensor concentration. The non-linear Michaelis-Menten fits were performed by the GraphPad prism software, and Michaelis-Menten parameters were calculated from the fits by the software. From the fit to the steady phase, the y-axis intercept was calculated.

For the data presented in figure 4, the slopes of the samples were compared directly. Calculated slopes were normalized to the mean of the first column in the chart to be able to show relative differences between the samples. Error bars represent standard deviation calculated from the triplicate experiments.

2.7 SDS gel electrophoreses and Coomassie staining

10% acrylamide gel electrophoresis was performed at 200V in SDS running buffer (25 mM Tris-HCl pH 7, 198 mM glycine, 0.1% w/v SDS) for 30-90 min. Prior to gel-loading, the protein samples were mixed with loading buffer (2% SDS, 2mM β-Mercapto-ethanol, 4% v/v Glycerol, 50 mM Tris-HCl pH 7, 0.05% w/v Bromophenol blue). PageRuler prestained Protein ladder from Thermo Scientific was used as a size marker. After gel electrophoresis, gels were fixed, stained with Coomassie Brilliant Blue and destained. Quantification of bands was done using the software Quantity One®.

2.8 DNA suicide substrate experiments

The DNA suicide substrate was composed of the oligonucleotides: 38SC: 5'-CTA GAG GAT CTA AAA GAC TTA GA-3' (23 bp), 26DL: 5'-pAGA AAA ATT TTT CCG AGT GCG AAG-3' (24 bp), 61NCL: 5'-CTT CGC ACT CGG AAA AAT TTT TCT AAG TCT TTT AGA TCC TCT AG-3' (44 bp). Note that the 26DL oligonucleotide was phosphorylated in the 5'-end to avoid religation. The three oligonucleotides were mixed in a 1:1:1 ratio forming the suicide substrate upon hybridization. The suicide substrate (2.5 µM final concentration) was mixed with purified hTopI (500 nM final concentration) in a 20 µL reaction volume in 1x hTopI buffer (10 mM Tris-HCl pH 7.5, 5 mM $CaCl_2$, 5 mM $MgCl_2$ and 0.1 mM DTT), and incubated for 30 min. at 37 ^{O}C. The reaction was stopped by addition of SDS and the reaction products were analyzed by coomassie 10% SDS polyacrylaminde gel electrophoresis.

2.9 Estimation of concentration of active hTopI using SDS gel electrophoresis

The total amount of hTopI in the purified stock fraction was calculated from coomassie stained gels by comparing the intensity of the band corresponding to hTopI with a titration of bovine serum albumin (BSA) with a known concentration (shown in supplementary figure 1).

To estimate the fraction of active enzyme in the stock, hTopI was incubated with an excess of the DNA suicide substrate, as described above, prior to analysis by 10% SDS polyacrylaminde gel electrophoresis. Covalent attachment of active hTopI to the DNA results in a gel-electrophoretic retardation, allowing the fraction of active and inactive enzyme to be determined after staining with coomassie brilliant blue by quantification of the bands. The result of such analyses is shown in supplementary figure 1.

3. Results and discussion:

3.1 DNA sensor assay design.

Figure 1A shows a schematic representation of the structure of the DNA sensor for hTopI used in this study. The sensor is composed of two oligonucleotides, which upon annealing form a nicked hairpin structure with the preferred hexadecameric recognition sequence for hTopI [35]. As shown by Marcussen et al. [2] and in

agreement with previous reports [35]–[37], hTopI cleaves the DNA sensor at the preferred cleavage site indicated with an arrow in figure 1A and only at this site. Upon cleavage, the generated tri-nucleotide with the quencher quickly diffuses away, resulting in an increase of fluorescence, which is the signal measured in the assay. Finally, the break is sealed by ligation of the free 5′-OH end of the second oligonucleotide of the substrate and the hTopI-DNA sensor complex dissociates. In this manner, the presented assay resembles traditional assays for measurement of topoisomerase IB cleavage-ligation activities, such as the one utilized for kinetic investigation of vvTopI [30], which measured the steady state catalysis by detection of a radiolabelled di-nucleotide (in principle similar to the quencher containing tri-nucleotide in this assay) generated during cleavage, while ligation was facilitated by addition of excess ligator DNA with a free 5′-OH.

The initial analyses of the DNA sensor demonstrated a burst profile, when it was incubated with hTopI at steady state conditions. As indicated in figure 1C the burst profile may be used to calculate important reaction constants as well as the active enzyme concentration.

The mechanistic scheme of the hTopI-DNA sensor burst reaction is shown in figure 1B. Here, k_{cl} is defined as the pre-steady state rate constant of cleavage, where the enzyme (E) converts the DNA sensor (S-Q) to the fluorescent product (P*). Q is the quencher-coupled trinucleotide that is cleaved off by hTopI. k_2 is the steady state rate constant of the catalytic steps subsequent to cleavage, including ligation, turnover, dissociation and association. This is consistent with the previous definition of the burst profile observed for vvTopI [30], except that in the vvTopI assay it was the dissociating di-nucleotide, (equivalent to Q in our assay) that was measured. Essentially, the mathematical basis of the burst phase analyses used here, relies on measurements of dissociation of the "leaving" moiety (Q) [29]. Due to limitations in the synthesis of modified DNA oligonucleotides, we chose to place the quencher at the leaving moiety and the fluorophore on the complex forming part of the DNA substrate. Thus in our assay, it is the formation of P* that is measured. However, since Q is generated simultaneously and in a 1:1 ratio to P*, the concentration of Q equals P* at all times. Note that the fluorescence of P* is detected both when P* is still in complex with hTopI (E-P*) and when P* is released.

From experimental data, it is possible to extract the reaction velocity (v) of the burst- and steady phases, respectively by performing a linear fit to the initial part of the burst phase and the steady state part of the steady phase [29]. When S-Q is in large excess the factor $\frac{[S-Q]}{[S-Q]+K_M}$ (see equations 1-2 in figure 1C) approximates 1 and, hence, the rate constant (k_{burst} and k_{steady}) can be calculated from v, given that the initial enzyme concentration, $[E]_0$, is known. Moreover, the equations in figure 1B shows that the burst amplitude can provide a value for the amount of active enzyme used in the reaction [29].

3.2. Investigation of the DNA sensor as a tool to determine enzymatic reaction rates.

In order to investigate if the described DNA sensor can be used for kinetic analyses of hTopI, the enzyme was incubated with different concentrations of the sensor in time course experiments, and the results registered in terms of fluorescent signals determined by a standard qPCR machine. Note here, that in principle any fluorescence reader capable of measuring fluorescence over time can be used for the readout. For determination of the rate constants (k_{steady} and k_{burst}), it is essential to know the concentration of active enzyme as indicated from equations 1-2 in figure 1C. Since hTopI may be inactivated by denaturation, post translational modifications or lack of modifications e.g. phosphorylations or oxidation, the total amount of enzyme does not necessarily equal the amount of active enzyme. Therefore, the amount of active hTopI in the utilized enzyme fraction was first determined. The concentration of total enzyme was estimated to 25 ng/µL by comparing to a titration of known concentrations of BSA in a comassie stained analytical SDS gel (data not shown). The percentage of active hTopI was estimated by incubation of 500 nM hTopI with a surplus (2.5 µM) of a DNA suicide substrate (see section 2.8). This substrate can be cleaved but not ligated by hTopI [36], [37] and, hence, active hTopI (which is able to cleave DNA) can be recognized by a band shift in a SDS gel due to covalent linkage to the DNA. In contrast, inactive hTopI does not change mobility upon incubation with the suicide substrate. Quantification of the bands appearing in a coomassie stained gel of such analyses (shown in figure 2A) demonstrated that approximately 80% of the enzyme in the fraction used (corresponding to 20 ng/µL) was active.

Figure 2B shows a representative example of the results obtained from a triplicate DNA sensor titration experiment, where 43 nM of active hTopI was added to samples containing varying DNA sensor concentrations ranging from 0.25-3 µM in a hTopI reaction buffer. The samples were incubated at a constant temperature of 37 °C and fluorescence was measured every 15 seconds using a qPCR machine. The amount of product corresponding to a given fluorescence was calculated using a conversion curve as explained in materials and methods (section 2.5).

As expected, incubation of the DNA sensor with hTopI resulted in a burst profile characterized by an initial steep increase in fluorescence (until around 1.5 min.), followed by a slower and linear increase in fluorescence (until at least 20 min.) representing the burst- and the steady phases, respectively. To calculate k_{burst}, linear least square fits were made to the initial points of the burst phases and the slopes were plotted as a function of DNA sensor concentrations (figure 2C). The maximal velocity of the burst phase (V_{max}^{burst}) and K_M (see table 1) was found by fitting the points in figure 2C to the Michaelis-Menten model using GraphPad Prism-software. From this k_{burst} could be calculated using equation 1. Note that according to Michaelis-Menten kinetics, the factor ($S/(S+K_M)$) in equation 1 equals 1 when v equals maximal velocity (V_{max}). The kinetic parameters for the steady phase (k_{steady} and K_M) were calculated as described above, except that a linear least square fit to the steady phase of the DNA sensor titration experiment curves (from 5-10 minutes) was used for the plot shown in figure 2D and calculation of the parameters. All the calculated parameters are shown in table 1.

Comparing our calculated K_M with the one reported by Stivers *et al.* for the interaction of vvTopI with a small double stranded substrate, the binding of hTopI to the sensor is around 10 fold weaker [30]. This difference may reflect the difference between DNA binding of the much smaller and more specific poxvirus topoisomerase and the larger less specific human enzyme. Also the presence of a quencher and a fluorophore situated close to or at the binding site of hTopI [17] in the utilized DNA sensor may add to weakening the K_M.

From the equations shown in figure 1C it is clear that simplifications can be made if $k_{cl} \gg k_2$. In such case $k_{steady} \approx k_2$ and $k_{burst} \approx k_{cl}$. This means that the rate constants k_{cl} and k_2 would correlate directly to the slope of

the burst- and steady phases, respectively, and that the concentration of active enzyme would equal the burst amplitude (see figure 1C). Calculation of k_{cl} and k_2 from equations 1 and 2 (see table 1) results in a ratio of k_{cl}/k_2 equal to 6.3. From this ratio, it is clear that k_{cl} is faster but not much faster than k_2, which implies that a certain error (~16%) must be expected if using assumptions that $k_{burst} \approx k_{cl}$ and $k_{steady} \approx k_2$. The reaction constants only change when the reaction conditions change, and as demonstrated below the burst phase profile can be used for accurate calculations of active enzyme concentrations in various reaction mixtures as long as the reaction conditions remain unaltered. Moreover, despite the error explained above, the rate of the burst phase and the rate of the steady phase may even be used for quick and easy approximations when analyzing changes in k_{cl} and k_2 due to difference in reaction conditions (see figure 4).

3.3 Calculating the amount of active hTopI from the burst amplitude

In theory, k_2 and k_{cl} remain unaltered when measuring different hTopI fractions using the same reaction conditions. Hence by knowing the amplification factor (AF), (which can be determined from k_2 and k_{cl} as shown in figure 1C), it is possible to calculate accurately the active enzyme concentration of different enzyme preparations using the DNA sensor. Such an approach presents the advantages of being relatively fast and easy to perform and requiring only very little enzyme compared to standard methods as the one shown in figure 2A.

To validate this assumption experimentally, we used the determined rate constants to calculate the amplification factor (AF) indicated in equation 3 in figure 1C (see table 1). Hereafter, increasing concentrations (ranging from 0-27 nM total amount of hTopI) of a new fraction of purified hTopI were incubated with the DNA sensor at steady state conditions using the same buffer condition as the one used in the experiments shown in figure 2B. The average results of triplicate experiments are shown in figure 3A. The amount of active enzyme in each sample was calculated as the burst phase amplitude divided by AF.

The concentration of active hTopI in the utilized enzyme preparation was determined by gel electrophoretic analyses of cleavage complexes as the one shown in figure 2A (data not shown). The results of the two different methods were compared in the plot shown in figure 3B, where the active hTopI concentrations

calculated by the use of the DNA sensor are plotted as a function of the active hTopI concentrations estimated by gel electrophoretic analysis. The linear fit has a slope of 1.082 (±0.091) suggesting a good agreement between the concentrations of active hTopI estimated by the two different methods.

The correlation between determinations of the active enzyme concentration using the sensor relative to traditional methods suggest that the DNA sensor may provide an easy alternative compared to the more laborious methods. Due to the high sensitivity, the sensor may be particularly useful for determination of active enzyme concentrations in extracts from cells or even human biopsies. Note, that we have previously demonstrated that the DNA sensor is specific for hTopI even in crude cell extracts [2]. As mentioned, since anticancer drugs act by stabilizing the hTopI cleavage complexes the concentration of active enzyme may be the important determinant of drug response. Provided that the AF is known, the absolute concentrations of active enzyme can readily be determined as in the example above. However, even when this factor is not known, a relative measure of active enzyme in different samples can be obtained using the DNA sensor, as described below.

3.4. Potential applications of the DNA sensor in drug screening.

hTopI is an important cellular target of several anticancer chemotherapeutics in clinical use or in trials. Unfortunately, many patients do not respond to treatment with these drugs and the search for new and more effective hTopI drugs continue. Screening for such new drugs is both time consuming and expensive. We therefore wanted to investigate if the DNA sensor can provide a tool for first line easy, fast and cost efficient investigation of new potential hTopI targeting drugs.

To diminish the experiment cost, a minimal amount of 1μM of the DNA sensor was used for these experiments. This concentration of DNA sensor (~20 times excess compared to enzyme) is sufficient to keep a reaction with 43 nM hTopI (which was the active enzyme concentration used in these experiments) at steady state within the first 20 minutes where the data were collected in the following experiments (note that the enzyme is very slow with 1 turnover per 18 minutes, table 1).

In the experimental setup, hTopI and DNA sensor at the stated concentrations were incubated in the presence 200 μM CPT or DMSO, which was used as a solvent for CPT, and the fluorescence was measured every 15 sec. as described above. The reaction rates of the burst- and steady phases were calculated as the slope of the linear fit to the burst phase and the steady phase as described for figures 2 and 3. As mentioned in section 3.2, since k_{cl} is only moderately faster than k_2 the calculated rates from the burst phase (v_{burst}) and the steady phase (v_{steady}) will be a relative approximation of the k_{cl} and k_2, respectively.

The measured reaction rates are shown in arbitrary units (a.u.) normalized to the control sample containing DMSO in figure 4A. As evident from the figure, the burst phase rates are unaffected by CPT while the rates of the steady phase are decreased upon addition of CPT. This is consistent with CPT inhibiting the catalytic steps subsequent to cleavage and suggests that the DNA sensor can be used not only to measure inhibition of hTopI but also to indicate the mechanism of drug action.

Further supporting the notion, that the burst phase rates can be regarded as an approximation to the rate of cleavage, while the steady phase rates provide an approximation for the steps succeeding cleavage, increasing the NaCl concentration of the reaction affected the steady phase rate, exclusively (figure 4B), which is consistent with NaCl primarily stimulating the dissociation step of hTopI catalyses [30], [38].

We anticipate that the DNA sensor may be used to investigate the effect of many other assay conditions on the hTopI cleavage-ligation reactions. However, conditions that prevent efficient hybridization of the fluorophore/quencher coupled DNA strands composing the DNA sensor such as omission of divalent cations cannot be investigated in the described assay setup (data not shown).

Conclusion:

The presented paper demonstrates the feasibility of a fluorophore and quencher coupled DNA sensor for studies of hTopI catalysis, including the action of hTopI inhibitors and equally important for determination of the concentration of active hTopI in various samples. The kinetic analysis of the hTopI reaction with the DNA sensor exhibits a characteristic burst profile, which was successfully used to calculate key reaction

constants of hTopI catalysis. The assay benefits from being easy to perform and to rely only on standard equipment available in most research- and clinical laboratories. Readout was done using a standard qPCR machine. However, any apparatus capable of measuring fluorescence emission as a function of time could be used. Since the burst reaction is a pre-steady state reaction, it is important to base calculations on linear fits at time points as close to zero as possible. This is practically difficult, using a qPCR machine due the lag time of this equipment and hence there is a risk of underestimating k_{burst}. Pointing towards the future, the introduction of new standard equipment, such as stopped-flow or microfluidic based setups, might be used to improve the fidelity of the data.

Besides its obvious benefits for basic science, the burst phase profile observed when incubating hTopI with the DNA sensor presents a fast and high throughput tool for dissecting the mechanism of action of potential new hTopI targeting anticancer drugs. Moreover, it presents a potential novel way to calculate the concentration of active hTopI in biological samples. hTopI is the sole cellular target of the anticancer therapeutics CPTs that act by trapping hTopI in covalent complex with DNA, which results in DNA damage and ultimately cell death. The cytotoxicity of CPT therefore correlates to the intracellular hTopI cleavage activity and, since only active enzymes can be trapped on DNA it seems reasonable to assume that also the fraction of active hTopI may be an important parameter for the effectiveness of CPT. Note here, that a high average hTopI activity can be caused by a small percentage of hyperactive hTopI and not necessarily reflect that a high fraction of the investigated hTopI population is active. The presented data suggest that the DNA sensor in short terms provides an effective tool to unravel the potential correlation between cellular CPT sensitivity and the intracellular concentration of active hTopI and in longer terms may be valuable for individualized cancer treatment with CPT derivatives.

List of abbreviations:

AF: Amplification factor. BHQ1: Black Hole Quencher 1. BSA: Bovine serum albumin. CPT: Camptothecin derivatives. [E0]: The amount of active enzyme added to the reaction. E-P*: The covalent hTopI-DNA sensor complex. E•S-Q: The non-covalent enzyme substrate complex. FAM: 6-carboxyfluorescein. hTopI: Human DNA topoisomerase I. k2: The first order rate constant of all reactions subsequent to cleavage. kbusrt: The rate constant of the burst phase. kcl: The first order rate constant of cleavage. KM: The Michaelis constant. ksteady: The rate constant of the steady phase. P*: The fluorescent product of the hTopI reaction on the DNA sensor. Q: The quencher-coupled trinucleotide that is cleaved off by hTopI. [S-Q]: The concentration of the DNA sensor. vburst: The initial velocity of the burst phase. vsteady: The steady state velocity of the steady phase. vvTopI: Vaccinia virus topoisomerase I

References:

[1]   P. W. Jensen, M. Falconi, E. L. Kristoffersen, A. T. Simonsen, J. B. Cifuentes, L. B. Marcussen, R. Frøhlich, J. Vagner, C. Harmsen, S. Juul, Y.-P. Ho, M. a Withers, J. R. Lupski, J. Koch, A. Desideri, B. R. Knudsen, and M. Stougaard, "Real-time detection of TDP1 activity using a fluorophore-quencher coupled DNA-biosensor.," *Biosens. Bioelectron.*, vol. 48C, pp. 230–237, Apr. 2013.

[2]   L. B. Marcussen, M. L. Jepsen, E. L. Kristoffersen, O. Franch, J. Proszek, Y.-P. Ho, M. Stougaard, and B. R. Knudsen, "DNA-based sensor for real-time measurement of the enzymatic activity of human topoisomerase I.," *Sensors (Basel).*, vol. 13, no. 4, pp. 4017–28, Jan. 2013.

[3]   M. L. Jepsen, A. Ottaviani, B. R. Knudsen, and Y.-P. Ho, "Quantum dot based DNA nanosensors for amplification-free detection of human topoisomerase I," *RSC Adv.*, vol. 4, no. 5, pp. 2491–2494, Dec. 2014.

[4]   A. H. Hardin, S. K. Sarkar, Y. Seol, G. F. Liou, N. Osheroff, and K. C. Neuman, "Direct measurement of DNA bending by type IIA topoisomerases: implications for non-equilibrium topology simplification.," *Nucleic Acids Res.*, vol. 39, no. 13, pp. 5729–43, Jul. 2011.

[5]   E. L. Kristoffersen, M. Gonzalez, M. Stougaard, and C. Tesauro, "Molecular Beacon Enables Combination of Highly Processive and Highly Sensitive Rolling Circle Amplification Readouts for Detection of DNA-Modifying Enzymes," *Nano Life*, p. 1541002, Nov. 2014.

[6]   U. Kettling, A. Koltermann, P. Schwille, and M. Eigen, "Real-time enzyme kinetics monitored by dual-color fluorescence cross-correlation spectroscopy," *Proc. Natl. Acad. Sci.*, vol. 95, no. 4, pp. 1416–1420, Feb. 1998.

[7]   A. Koltermann, U. Kettling, J. Bieschke, T. Winkler, and M. Eigen, "Rapid assay processing by integration of dual-color fluorescence cross-correlation spectroscopy: High throughput screening for enzyme activity," *Proc. Natl. Acad. Sci.*, vol. 95, no. 4, pp. 1421–1426, Feb. 1998.

[8]   J. Deng, Y. Jin, L. Wang, G. Chen, and C. Zhang, "Sensitive detection of endonuclease activity and inhibition using gold nanorods.," *Biosens. Bioelectron.*, vol. 34, no. 1, pp. 144–50, Apr. 2012.

[9]   R. A. Katz, G. Merkel, M. D. Andrake, H. Roder, and A. M. Skalka, "Retroviral integrases promote fraying of viral DNA ends.," *J. Biol. Chem.*, vol. 286, no. 29, pp. 25710–8, Jul. 2011.

[10]   S. Lee, S.-R. Jung, K. Heo, J. A. W. Byl, J. E. Deweese, N. Osheroff, and S. Hohng, "DNA cleavage and opening reactions of human topoisomerase IIα are regulated via Mg2+-mediated dynamic bending of gate-DNA.," *Proc. Natl. Acad. Sci. U. S. A.*, vol. 109, no. 8, pp. 2925–30, Feb. 2012.

[11]   H.-H. Lin and C.-Y. Huang, "Characterization of flavonol inhibition of DnaB helicase: real-time monitoring, structural modeling, and proposed mechanism.," *J. Biomed. Biotechnol.*, vol. 2012, p. 735368, Jan. 2012.

[12]   V. Metelev, S. Zhang, D. Tabatadze, and A. Bogdanov, "Hairpin-like fluorescent probe for imaging of NF-κB transcription factor activity.," *Bioconjug. Chem.*, vol. 22, no. 4, pp. 759–65, Apr. 2011.

[13]   E. Noble, A. Cox, J. Deval, and B. Kim, "Endonuclease substrate selectivity characterized with full-length PA of influenza A virus polymerase.," *Virology*, vol. 433, no. 1, pp. 27–34, Nov. 2012.

[14]   "Quantitative, real-time analysis of base excision repair activity in cell lysates utilizing lesion-specific molecular beacons.," *J. Vis. Exp.*, no. 66, p. e4168, Jan. 2012.

[15]   Y.-H. Hsiang, M. G. Lihou, and L. F. Liu, "Arrest of Replication Forks by Drug-stabilized Topoisomerase I-DNA Cleavable Complexes as a Mechanism of Cell Killing by Camptothecin," *Cancer Res.*, vol. 49, no. 18, pp. 5077–5082, Sep. 1989.

[16]   H. Zhang, J. C. Wang, and L. F. Liu, "Involvement of DNA topoisomerase I in transcription of human ribosomal RNA genes.," *Proc. Natl. Acad. Sci.*, vol. 85, no. 4, pp. 1060–1064, Feb. 1988.

[17]   L. Stewart, "A Model for the Mechanism of Human Topoisomerase I," *Science (80-.).*, vol. 279, no. 5356, pp. 1534–1541, Mar. 1998.

[18]   J. J. Champoux, "DNA topoisomerases: structure, function, and mechanism.," *Annu. Rev. Biochem.*, vol. 70, pp. 369–413, Jan. 2001.

[19]   J. C. Wang, "Cellular roles of DNA topoisomerases: a molecular perspective," *Nat Rev Mol Cell Biol*, vol. 3, no. 6, pp. 430–440, Jun. 2002.

[20]   S. H. Chen, N.-L. Chan, and T. Hsieh, "New mechanistic and functional insights into DNA topoisomerases.," *Annu. Rev. Biochem.*, vol. 82, pp. 139–70, Jan. 2013.

[21]   S. Ogino, K. Shima, J. A. Meyerhardt, N. J. McCleary, K. Ng, D. Hollis, L. B. Saltz, R. J. Mayer, P. Schaefer, R. Whittom, A. Hantel, A. B. Benson, D. Spiegelman, R. M. Goldberg, M. M. Bertagnolli, and C. S. Fuchs, "Predictive and prognostic roles of BRAF mutation in stage III colon cancer: results from intergroup trial CALGB 89803.," *Clin. Cancer Res.*, vol. 18, no. 3, pp. 890–900, Feb. 2012.

[22]   C. D. Yeo, S. H. Lee, J. S. Kim, S. J. Kim, S. C. Kim, Y. K. Kim, H. H. Kang, H. K. Yoon, J. S. Song, H. S. Moon, J. W. Kim, K. H. Kim, B. Y. Shim, and C. H. Kim, "A multicenter phase II study of belotecan, a new camptothecin analogue, in elderly patients with previously untreated, extensive-stage small cell lung cancer.," *Cancer Chemother. Pharmacol.*, vol. 72, no. 4, pp. 809–14, Oct. 2013.

[23]   L. B. Saltz, J. V. Cox, C. Blanke, L. S. Rosen, L. Fehrenbacher, M. J. Moore, J. A. Maroun, S. P. Ackland, P. K. Locker, N. Pirotta, G. L. Elfring, and L. L. Miller, "Irinotecan plus fluorouracil and leucovorin for metastatic colorectal cancer. Irinotecan Study Group.," Massachusetts Medical Society, 2000.

[24]   R. F. Ozols, "Optimum chemotherapy for ovarian cancer," *Int. J. Gynecol. Cancer*, vol. 10, no. s1, pp. 33–37, Jan. 2000.

[25]   Y. Hsiang, R. Hertzberg, S. Hecht, and L. Liu, "Camptothecin induces protein-linked DNA breaks via mammalian DNA topoisomerase I," *J. Biol. Chem.*, vol. 260, no. 27, pp. 14873–14878, Nov. 1985.

[26]   T. Furuta, H. Takemura, Z.-Y. Liao, G. J. Aune, C. Redon, O. A. Sedelnikova, D. R. Pilch, E. P. Rogakou, A. Celeste, H. T. Chen, A. Nussenzweig, M. I. Aladjem, W. M. Bonner, and Y. Pommier, "Phosphorylation of histone H2AX and activation of Mre11, Rad50, and Nbs1 in response to replication-dependent DNA double-strand breaks induced by mammalian DNA topoisomerase I cleavage complexes.," *J. Biol. Chem.*, vol. 278, no. 22, pp. 20303–12, May 2003.

[27]   I. Nielsen, I. B. Bentsen, M. Lisby, S. Hansen, K. Mundbjerg, A. H. Andersen, and L. Bjergbaek, "A Flp-nick system to study repair of a single protein-bound nick in vivo.," *Nat. Methods*, vol. 6, no. 10, pp. 753–7, Oct. 2009.

[28]   A. G. Marangoni, *Enzyme Kinetics: A Modern Approach*. John Wiley & Sons, 2003, pp. 90–102.

[29]   A. R. Fersht, *Enzyme Structure and Mechanism*, 2nd ed. W. H. Freeman & Co., New York, 1985, pp. 143–144.

[30]   J. T. Stivers, S. Shuman, and a S. Mildvan, "Vaccinia DNA topoisomerase I: single-turnover and steady-state kinetic analysis of the DNA strand cleavage and ligation reactions.," *Biochemistry*, vol. 33, no. 1, pp. 327–39, Jan. 1994.

[31]   M. Lisby, B. O. Krogh, F. Boege, O. Westergaard, and B. R. Knudsen, "Camptothecins inhibit the utilization of hydrogen peroxide in the ligation step of topoisomerase I catalysis.," *Biochemistry*, vol. 37, no. 30, pp. 10815–27, Jul. 1998.

[32]   M.-A. Bjornsti, P. Benedetti, G. A. Viglianti, and J. C. Wang, "Expression of Human DNA Topoisomerase I in Yeast Cells Lacking Yeast DNA Topoisomerase I: Restoration of Sensitivity of the Cells to the Antitumor Drug Camptothecin," *Cancer Res.*, vol. 49, no. 22, pp. 6318–6323, Nov. 1989.

[33] B. R. Knudsen, T. Straub, and F. Boege, "Separation and functional analysis of eukaryotic DNA topoisomerases by chromatography and electrophoresis," *J. Chromatogr. B Biomed. Sci. Appl.*, vol. 684, no. 1–2, pp. 307–321, Sep. 1996.

[34] M. S. Hede, R. L. Petersen, R. F. Frøhlich, D. Krüger, F. F. Andersen, A. H. Andersen, and B. R. Knudsen, "Resolution of Holliday junction substrates by human topoisomerase I.," *J. Mol. Biol.*, vol. 365, no. 4, pp. 1076–92, Jan. 2007.

[35] A. H. Andersen, E. Gocke, B. J. Bonven, O. F. Nielsen, and O. Westergaard, "Topoisomerase I has a strong binding preference for a conserved hexadecameric sequence in the promotor region of the rRNA gene from Tetrahymena pyriformis," *Nucleic Acids Res.*, vol. 13, no. 5, pp. 1543–1557, Mar. 1985.

[36] K. Christiansen and O. Westergaard, "Characterization of intra- and intermolecular DNA ligation mediated by eukaryotic topoisomerase I. Role of bipartite DNA interaction in the ligation process.," *J. Biol. Chem.*, vol. 269, no. 1, pp. 721–9, Jan. 1994.

[37] K. Christiansen, A. B. Svejstrup, A. H. Andersen, and O. Westergaard, "Eukaryotic topoisomerase I-mediated cleavage requires bipartite DNA interaction. Cleavage of DNA substrates containing strand interruptions implicates a role for topoisomerase I in illegitimate recombination.," *J. Biol. Chem.*, vol. 268, no. 13, pp. 9690–701, May 1993.

[38] S. Shuman and J. Prescott, "Specific DNA cleavage and binding by vaccinia virus DNA topoisomerase I.," *J. Biol. Chem.*, vol. 265, no. 29, pp. 17826–17836, Oct. 1990.

Figure legends:

Table 1

The calculated reaction constants for the reaction conditions described in the text.

Figure 1

(A) The sequence and structure of the DNA sensor. The colored circles, F and Q, represent the internally attached fluorophore (FAM) and 3'-attached Black Hole Quencher 1 (BHQ1), respectively. The hTopI cleavage site is indicated by an arrow. (B) The schematic presentation of the hTopI reaction with the DNA sensor. E denotes the hTopI enzyme, S-Q denotes the DNA sensor in its quenched form. E•S-Q is the non-covalent enzyme substrate complex. Upon enzymatic cleavage, a tri-nucleotide with the quencher (Q) is cleaved off leading to formation of a covalent hTopI-DNA sensor complex (E-P*). The asterisk indicates the recovered fluorescence. k_{cl} denotes the rate of cleavage, k_2 denotes the rate of the substrate turnover subsequent to the cleavage. During the timescale where data are collected, up to 10 minutes, both reactions are considered one way reactions. (C) Schematic representation of the burst profile with the equations describing the reaction (modified from [29]).

Figure 2

(A) Gel electrophoretic analysis of an hTopI cleavage reaction followed by standard coomassie stain. Lane 1, size marker, lane 2, hTopI cleavage reaction. Right panel, schematic illustration of reaction products visualized in the gel i.e. hTopI (Tp) in complex with DNA (top) and free hTopI (bottom). A quantification of the bands representing hTopI-DNA complexes and free hTopI is indicated below the gel picture. (B) The average of three experiments where hTopI was incubated with the indicated concentrations of the sensor and measured over time. The results are shown as the concentration of product formed plotted as a function of time. From these data, the reaction rates were calculated. (C) A classical Michaelis-Menten plot for the burst phase in which the rates of the burst phase are plotted as a function of sensor concentrations. (D) Same as (C) except that these data represent the steady phase. Standard error of the mean of three independent experiments are indicated in (C) and (D).

Figure 3

(A) The average of three experiments where the indicated concentrations of active hTopI were incubated with 1 μM sensor. The amounts of product formed are plotted as a function of incubation time. (B) The concentrations of active hTopI in five different samples calculated by using the sensor assay are plotted as a function of the concentrations of active hTopI in similar samples calculated using a tradition gel-based assay. The error bars in (B) indicate standard derivations of three independent experiments.

Figure 4

(A) Reaction rate of the burst phase (left) and the steady phase (right) observed when hTopI was incubated with the sensor in the absence or presence of 200 μM CPT. Results are normalized to the sample without CPT. (B) Same as (A) except that CPT was replaced by 150 mM NaCl. The experiments were performed in triplicates and error bars represent standard deviation.

Table 1, Michaelis-Menten (best fit values)
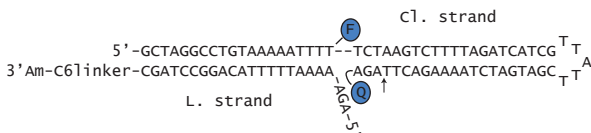Kinetic parameters for hTopI (43 nM) on the DNA sensor

Burst Phase

Vmax (μM/min):   0.02102 ($\pm$0.002656)

Km (μM):   0.4691 ($\pm$0.2171)

k_{burst}(1/s):   80 ($\pm$10) x10^-4

Steady phase

Vmax (μM/min.):   0.002479 ($\pm$0.000250)

Km (μM):   0.4659 ($\pm$0.1731)

k_{steady}(1/s):   9.5 ($\pm$0.95) x10^-4

Reaction rate constants

k_{cl}(1/s):   69 x10^-4

k_2 (1/s):   11 x10^-4

AF[*] (TopI buffer, 37 $^{\circ}$C): 0.86

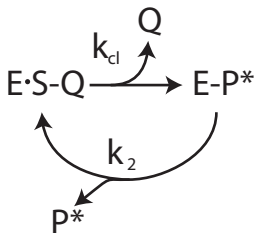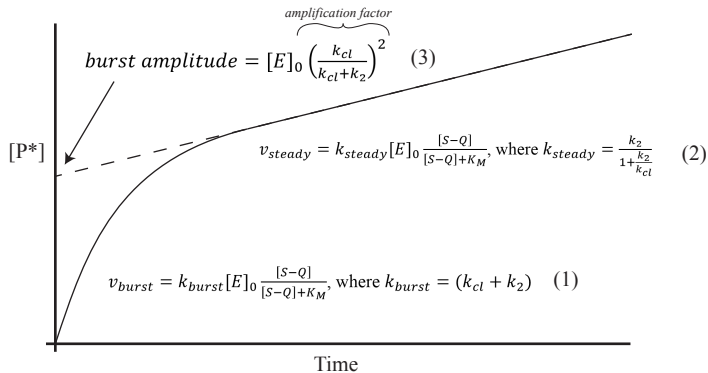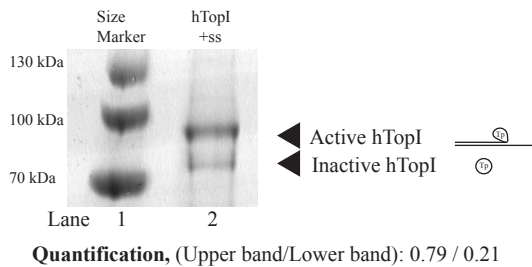[*] Amplification factor (AF) is calculated from k_{cl} and k_2 as seen from equation 3 in figure 1

Figure 1 **Nanoscale** **Page 24 of 27**

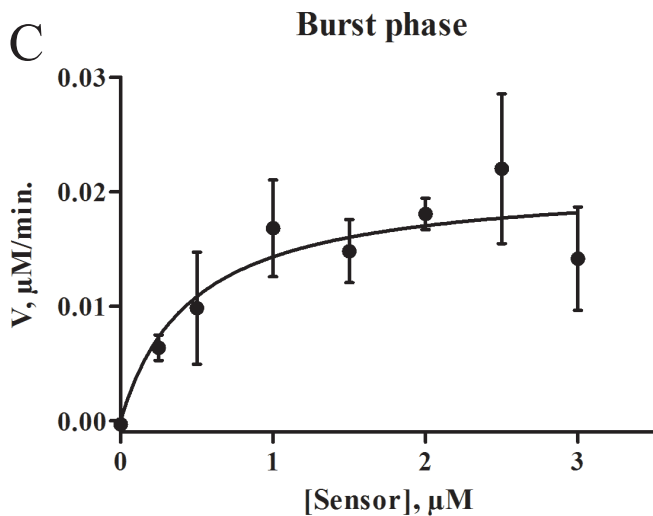
A

```
                                              F    Cl. strand
5'-GCTAGGCCTGTAAAAATTTT--TCTAAGTCTTTTAGATCATCG^T^T
3'Am-C6linker-CGATCCGGACATTTTTAAAA AGATTCAGAAAATCTAGTAGC^T^T^A
                                    AGA-5'   Q
                              L. strand    ↑
```

B

$$E \cdot S\text{-}Q \xrightarrow{\;k_{cl}\;} E\text{-}P^*$$

with Q released, and k_2 releasing P^*.

C

$$\text{burst amplitude} = [E]_0 \left(\frac{k_{cl}}{k_{cl}+k_2}\right)^2 \quad (3)$$

amplification factor

$$v_{steady} = k_{steady}[E]_0 \frac{[S\text{-}Q]}{[S\text{-}Q]+K_M}, \text{ where } k_{steady} = \frac{k_2}{1+\frac{k_2}{k_{cl}}} \quad (2)$$

$$v_{burst} = k_{burst}[E]_0 \frac{[S\text{-}Q]}{[S\text{-}Q]+K_M}, \text{ where } k_{burst} = (k_{cl}+k_2) \quad (1)$$

[P*]

Time

Figure 2

A

Quantification, (Upper band/Lower band): 0.79 / 0.21

B

Substrate titration

[DNA sensor]
- 3 μM
- 2.5 μM
- 2 μM
- 1.5 μM
- 1 μM
- 0.5 μM
- 0.25 μM
- 0 μM

C

Burst phase

D

Steady phase

Figure 3

A

hTopI dilutions

[Active hTopI]
- 27.3 nM
- 18.2 nM
- 9.1 nM
- 4.5 nM
- 2.3 nM
- 0 nM

B

Slope: 1.082 (±0.09)

Nanoscale

Figure 4

A

Burst phase

Steady phase

B

Burst phase

Steady phase